ELSEVIER

Thermochimica Acta 307 (1997) 37–43

thermochimica acta

The dehydration schemes of rare-earth chlorides

Vu Van Hong[1], Johan Sundström*

Division of Process Metallurgy, The Royal Institute of Technology, S-100 44 Stockholm, Sweden

Received 14 March 1997; accepted 16 June 1997

Abstract

The dehydration schemes of $LaCl_3 \cdot 7H_2O$, $CeCl_3 \cdot 7H_2O$, $PrCl_3 \cdot 7H_2O$, $SmCl_3 \cdot 6H_2O$, $EuCl_3 \cdot 6H_2O$, $GdCl_3 \cdot 6H_2O$, $HoCl_3 \cdot 6H_2O$, $ErCl_3 \cdot 6H_2O$, $TmCl_3 \cdot 6H_2O$, $YbCl_3 \cdot 6H_2O$ and $YCl_3 \cdot 6H_2O$ have been investigated by the isothermal fluidized-bed technique. This technique is based on the fact that reactions proceed at a close approach to equilibrium and thus give rise to constant reaction rate regimes at constant gas flow and temperature in the bed. By injecting a small portion of HCl(g) (~1%) into the gas stream, hydrolysis is avoided, and dehydration to the monohydrate is recorded by both thermal analysis of the preheated inlet gas and chemical analysis of samples taken from the bed. Based on the present results, together with previous results on $NdCl_3 \cdot 6H_2O$, $TbCl_3 \cdot 6H_2O$ and $DyCl_3 \cdot 6H_2O$, dehydration schemes of all rare-earth chlorides except $LuCl_3$ and $ScCl_3$ are suggested. © 1997 Elsevier Science B.V.

Keywords: Dehydration; Fluidized bed; Hydrates; Rare-earth chlorides

1. Introduction

Knowledge of the dehydration schemes of rare-earth chlorides is important if the anhydrous state is produced by a dehydration process. In a fluidized-bed process, the different reaction steps strongly influence the reaction rate and it may be useful to correlate the behaviour of the reacting system with the dehydration scheme [1]. Anhydrous rare-earth chlorides are attractive precursor compounds for producing mischmetal and the low-melting metals lanthanum and cerium. They are also used to produce low-melting master alloys of important bulk alloys, such as NdFe [2,3]. Some research has pointed out the possibility of using anhydrous rare-earth chlorides in electrodeposition processes for producing protective surface layers of rare-earth intermetallics [4]. These processes depend on alloy diffusion in the solid state and therefore are not limited by the melting point of the rare-earth metal.

Previous work [5] has shown the possibility of using the fluidized bed as a reactor to study dehydration reactions. By adding a sufficient flow of HCl to the dry gas stream, hydrolysis was avoided and the trichloride structure was preserved. The fluidized-bed technique possesses many advantages compared to fixed-bed techniques. The most important are: (1) turbulent mixing particles; (2) outstanding heat transfer characteristics; and (3) plenty enough powder can be charged and frequent sampling of powder may be done without disturbing the thermochemical conditions in the bed (provided that a tiny sampler is used).

*Corresponding author. Present address: Höganäs AB (Publ.), Research & Development, S-26383 Höganäs, Sweden. Tel.: +46 42 33 8639; Fax: +46 42 338188; e-mail: johan.sundstrom@hoganas.com

[1]Present address: Department of Rare Earth Metals, Institute of Materials Science, NCST, Nghia do, Tu liem, Hanoi, Vietnam.

PII S0040-6031(97)00296-7

The first stated advantage serves for complete access of HCl around the particles; the second stated advantage enables the use of an isothermal technique; and the third stated advantage signifies the possibility of using two reciprocally independent means to analyze the dehydration reactions, viz. chemical analysis of samples and thermal analysis of the preheated inlet gas. However, the most important advantage is related to the nature of dehydration kinetics, which has been shown favourable enough to serve for pseudo equilibrium conditions in the bed [6]; in other words, the overall rate-limiting factor in the fluidized-bed process is the transport of gaseous water by bulk gas flow. Consequently, the reaction rate is a function of only two parameters: temperature and gas-flow rate. Keeping both constant renders a constant reaction rate, except during the transient periods around the stable hydrates where the change to a new (or cease of) reaction occurs. After such a breakpoint, the equilibrium vapour pressure is reduced to the next lower reaction step which correspondingly reduces the dehydration rate. This behaviour was first discovered by the experiments worked out in [5] on Nd-, Tb- and $DyCl_3 \cdot 6H_2O$, and has been consistent throughout all the experiments in this work as well.

The first comprehensive study of the thermal decomposition of hydrated rare-earth chlorides was made by Wendlandt [7,8]. He used a thermobalance and heated the samples at a rate of 5.4°C/min in an atmosphere of air. Both the high-heating rate and the use of a HCl-free atmosphere could explain that no intermediate hydrates before the monohydrate were observed. Powel and Burkholder [9] were able to disclose $LaCl_3 \cdot 7H_2O$, $LaCl_3 \cdot 3H_2O$, $LaCl_3 \cdot H_2O$ and $LaCl_3$ by slowly heating samples of 0.5–1.0 g in a thermobalance until a weight loss was observed, then holding the temperature constant until the reaction had completed. $LaCl_3 \cdot 6H_2O$ was not detected from the weight loss curve, but was disclosed as crystals precipitated from a hot saturated solution. Haeseler and Matthes [10] also used a thermobalance in their comprehensive investigation, but they improved the thermochemical conditions for dehydration by adding HCl to the atmosphere. This enabled them to study the dehydration schemes of the heavier rare-earth chlorides without obtaining deleterious hydrolysis. Ashcroft and Mortimer [11] used a differential scanning calorimeter to investigate the intermediate dehydration steps of all hydrated lanthanide chlorides during their thermal decomposition in a nitrogen atmosphere. Su and Li [12] used a static membrane method to follow the pressure increase during the thermal decomposition of hydrated rare-earth chlorides and their dehydration schemes were derived from these data. Ukraintseva et al. [13–15] followed the dehydration by non-isothermal thermogravimetry of hydrated rare-earth chlorides placed in crucibles with lids. Only the first dehydration step was considered. Wang et al. [16] prepared the trihydrates of some rare-earth chlorides and followed the dehydration of these by non-isothermal thermogravimetry in a flow of nitrogen. Kipouros and Sharma [17] used DTA to investigate the dehydration of $NdCl_3 \cdot 6H_2O$. The results of all cited investigations are summarized in Table 2.

The aim of the present paper is to report the dehydration schemes of all rare-earth chlorides (except Pm-, Lu- and $ScCl_3$) based on the fluidized-bed technique. Since there seems to be no controversy regarding the last reaction step of dehydration ($1 \rightarrow 0$), the dehydration of the monohydrate was not investigated in this work.

2. Experimental

2.1. Materials

Rare-earth oxides with purities listed in Table 1 were supplied by Rhône Poulenc Chimie, France. Hydrated $CeCl_3$ and $HoCl_3$ of 99.9% were supplied by Alfa (a Johnson Matthey). Argon of 99.996% purity (<5ppm H_2O and <5ppm O_2) and hydrogen chloride gas of 99.995% purity were supplied by AGA Gas AB, Sweden.

2.2. Equipment and procedure

Distilled water and hydrochloric acid (Pro Analysi) were used to dissolve the oxides into clear solutions. Excess water was boiled off during constant stirring

Table 1
Purities of rare-earth oxides supplied by Rhône Poulenc Chimie

La	Pr	Sm	Eu	Gd	Er	Tm	Yb	Y
99.9	99.9	98	99.99	99.9	99.9	99.9	99	99.9

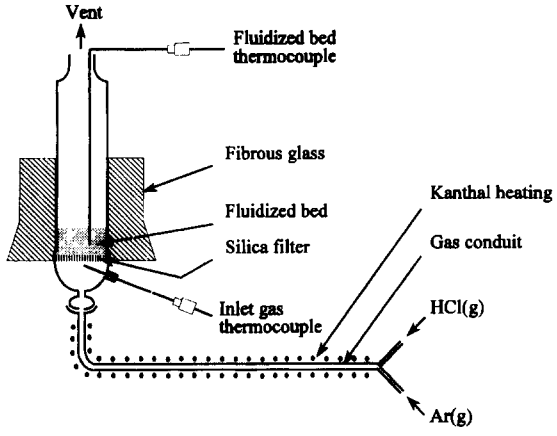

Fig. 1. Schematic picture of the experimental assembly.

and hydrated rare-earth chloride crystals were precipitated until a thick slurry was obtained. After the slurry had been cooled to room temperature, remaining excess solution was filtered off. The solid product was vacuum-treated (<1 torr) at 30–40°C in order to remove excess water. Grinding and stirring were conducted at intervals to finally obtain a completely dry and sievable hydrated rare-earth chloride product. For those chlorides which form heptahydrates, viz. La-, Ce- and $PrCl_3$, the dehydration of crystallized water occurred with this treatment. Therefore, they were rehydrated up to z=6.9–7.0 in an atmosphere of increased humidity under frequent stirring. The hydration number was conveniently controlled by a reference analysis followed by weighing. The final powder was seived to obtain a particle size distribution between 150 and 355 μm.

Fluidization was carried out with the equipment shown in Fig. 1. The gas conduit and the fluidization tube were made of Pyrex glass. The fluidization tube measured 50 mm in inside diameter and 400 mm in height. The gas stream was heated before entering into the fluidization tube by a Kanthal wire wound around the gas conduit. The temperature was measured by Chromel–Alumel (type K) thermocouples at two positions: (1) in the inlet gas stream before the silica filter and (2) in the fluidized bed. The bed temperature was controlled by a PID-regulator. In order to keep it constant the heating power was regulated in accordance with the heat-consumption rate in the fluidized bed (viz. the dehydration rate). The inlet gas temperature, which varied according to the heating power, was recorded continuously. In order to minimize temperature drop near the walls of the tube, the outer walls were insulated with fibrous glass. The thermal homogeneity of the bed was within ±0.2°C. Turbulent mixing of particles and homogeneous temperature distribution were ensured by carrying out fluidization in the vigorously bubbling state. The gas-flow rate of Ar was measured with a flow meter to an accuracy within ±5%. The gas-flow rate of HCl was fixed to 0.1±0.02 l/min, which corresponded to about 1% of the inlet gas composition. Each experiment began by manually regulating the heating power up to the desired bed temperature. The power was then adjusted to maintain a fairly constant temperature around the aimed value. After this target was reached, automatic regulation was set on, using the PID-parameters previously calculated by the Self-tune program at similar processing conditions. The first sample was taken as soon as the temperature became constant with time. A small glass cup suspended from a steel wire functioned as a sampler. Samples, weighing about 400 mg, were quickly put into 15 ml jars with tightly-sealed screw caps and stored in a desiccator before analysis. Analysis of chlorine was made by the gravimetric silver chloride method. The molar water content, z ($RCl_3 \cdot zH_2O$), was calculated from the chlorine content of the sample. The uncertainty in this method has been estimated to $\Delta z = \pm 0.002$. However, a necessary prerequisite for the precision given is that samples are free of hydrolytic compounds, which if present are easily detected as insoluble particles in the analytical solution. Because of the establishment of 1% partial pressure of HCl in the fluidized-bed atmosphere, all samples formed 'crystal clear' solutions in water, proving that hydrolysis was absent.

3. Results and discussion

Starting compounds were $LaCl_3 \cdot 7H_2O$, $CeCl_3 \cdot 7H_2O$, $PrCl_3 \cdot 7H_2O$, $SmCl_3 \cdot 6H_2O$, $EuCl_3 \cdot 6H_2O$, $GdCl_3 \cdot 6H_2O$, $HoCl_3 \cdot 6H_2O$, $ErCl_3 \cdot 6H_2O$, $TmCl_3 \cdot 6H_2O$, $YbCl_3 \cdot 6H_2O$ and $YCl_3 \cdot 6H_2O$. In average, about three experiments were conducted for each compound, using 28–40 g of powder each time. The total gas flow was in the range 12–14 l/min in all experiments. Figs. 2–12 show the plots which best illustrate the dehydration scheme of

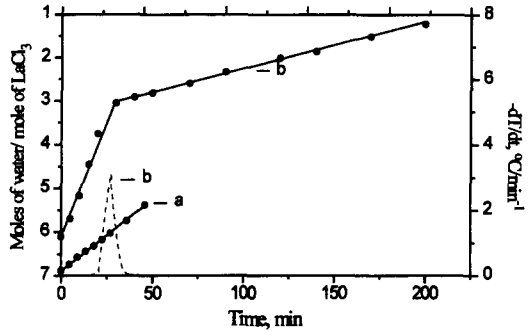

Fig. 2. Dehydration of $LaCl_3 \cdot 7H_2O$. (a) m_0=28 g; Δd_p=180–250 μm; Q=13.1 l min^{-1}; T=35°C. (b) m_0=35 g; Δd_p=180–355 μm; Q=12.5 l min^{-1}; T=60°C.

each specific compound. The analyzed H_2O-content of samples taken during dehydration have been plotted in the diagrams. Straight lines have been adapted to the periods of constant reaction rate in order to mark this behaviour. The time differential of the inlet gas temperature on the right ordinate is plotted against time and its peaks coincide with the breakpoints of transient periods occurring around the stable hydrates.

In order to obtain the complete dehydration scheme, it was in some cases necessary to perform two experiments at different temperatures. These have been referred to as 'a' and 'b' in Figs. 2–4, 10, 11. It is interesting to see that La-, Ce- and $PrCl_3 \cdot 7H_2O$ required very low temperatures (35, 30 and 32°C, respectively) to enable investigation of the dehydration between z=7 and 6. The sticky behaviour of powder in this compositional range impaired the fluidizability and could easily cause the bed to col-

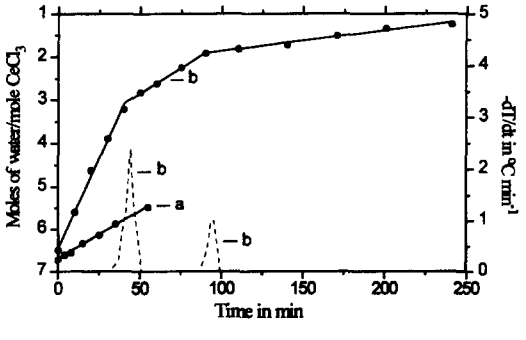

Fig. 3. Dehydration of $CeCl_3 \cdot 7H_2O$. (a) m_0=29 g; Δd_p=150–250 μm; Q=13.1 l min^{-1}; T=30°C. (b) m_0=35 g; Δd_p=180–355 μm; Q=12.5 l min^{-1}; T=55°C.

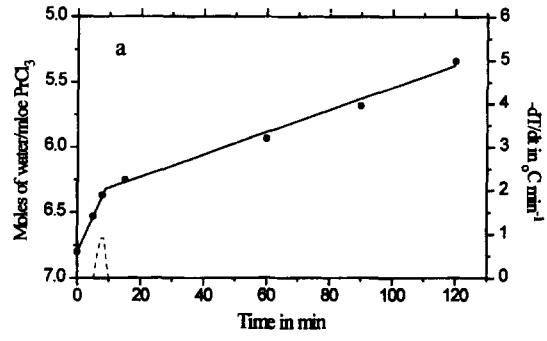

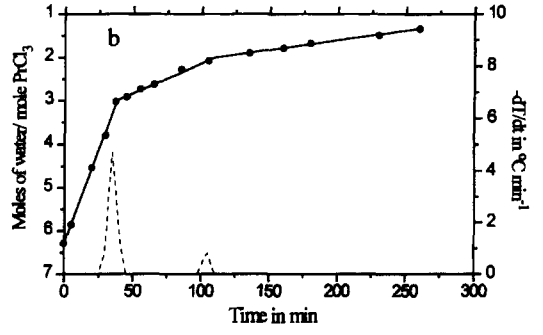

Fig. 4. Dehydration of $PrCl_3 \cdot 7H_2O$. (a) m_0=28 g; Δd_p=180–250 μm; Q=13.1 l min^{-1}; T=32°C. (b) m_0=34 g; Δd_p=180–355 μm; Q=12.5 l min^{-1}; T=65°C.

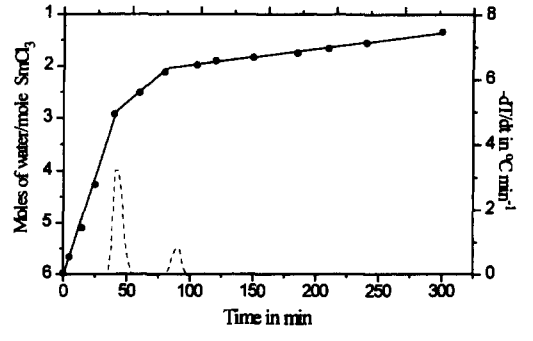

Fig. 5. Dehydration of $SmCl_3 \cdot 6H_2O$. m_0=28 g; Δd_p=150–355 μm; Q=12.5 l min^{-1}; T=75°C.

lapse with gas passing through the channels. Satisfactory conditions were obtained by decreasing and narrowing the particle fraction and subsequently flushing (30–40 l/min) it for a few minutes at room temperature (~15°C). The last treatment was particularly efficient since it removed most of the adhesive dust, which otherwise was impossible to remove by sieving.

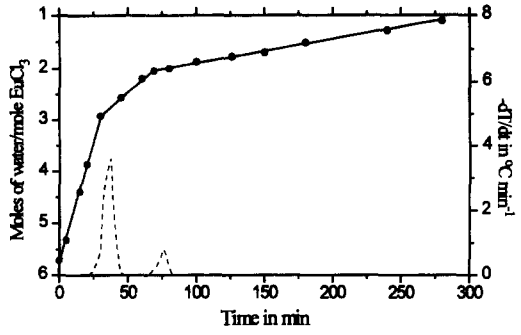

Fig. 6. Dehydration of $EuCl_3 \cdot 6H_2O$. m_0=34 g; Δd_p=180–355 μm; Q=13.5 l min^{-1}; T=80°C.

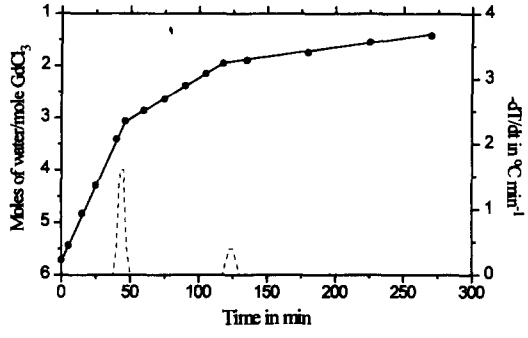

Fig. 7. Dehydration of $GdCl_3 \cdot 6H_2O$. m_0=34 g; Δd_p=180–355 μm; Q=13.4 l min^{-1}; T=75°C.

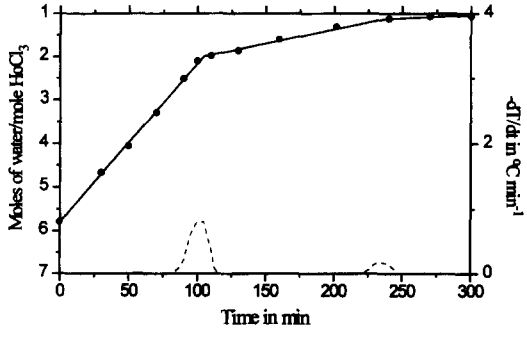

Fig. 8. Dehydration of $HoCl_3 \cdot 6H_2O$. m_0=34 g; Δd_p=180–355 μm; Q=13.4 l min^{-1}; T=85°C.

Most of the results in Figs. 2–12 seem very clear and easy to interpret as specific dehydration schemes of integer of hydrates. For example, the results of $LaCl_3 \cdot 7H_2O$ in Fig. 2 show that only one breakpoint occurs at z=3. No breakpoint was observed at $z \geq 6$, which is particularly evidenced by the experiment at

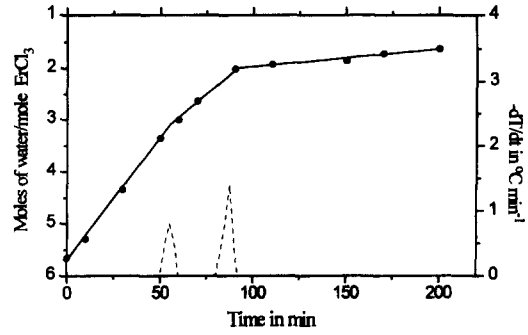

Fig. 9. Dehydration of $ErCl_3 \cdot 6H_2O$. m_0=34 g; Δd_p=180–355 μm; Q=12.5 l min^{-1}; T=85°C.

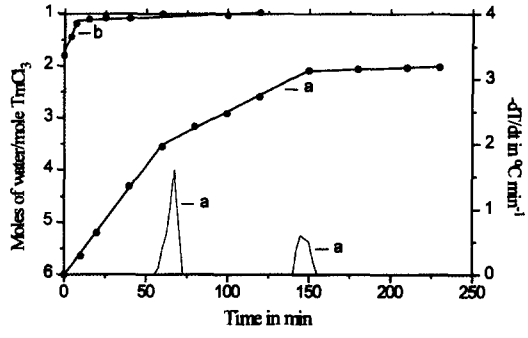

Fig. 10. Dehydration of $TmCl_3 \cdot 6H_2O$. (a) m_0=34 g; Δd_p=150–355 μm; Q=12.5 l min^{-1}; T=80°C. (b) m_0=32 g; Δd_p=150–250 μm; Q=12.5 l min^{-1}; T=135°C.

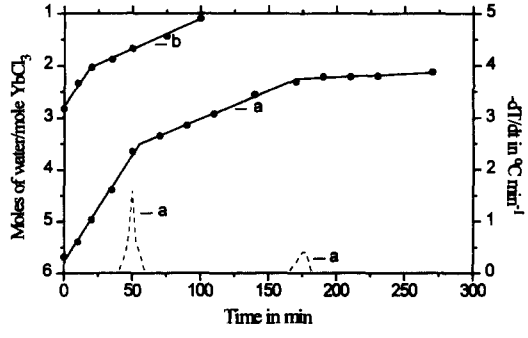

Fig. 11. Dehydration of $YbCl_3 \cdot 6H_2O$. (a) m_0=34 g; Δd_p=150–355 μm; Q=12.5 l min^{-1}; T=80°C. (b) m_0=34 g; Δd_p=150–355 μm; Q=12.5 l min^{-1}; T=105°C.

35°C. Thus, the dehydration scheme of $LaCl_3 \cdot 7H_2O$ is: 7→3→1. However, some other results are not as easy to interpret and require discussion as follows. The dehydration of $PrCl_3 \cdot 7H_2O$ shows an anomalous

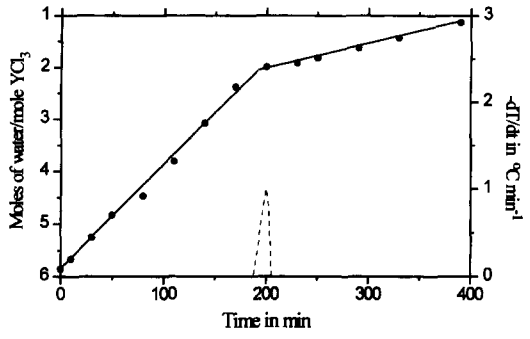

Fig. 12. Dehydration of $YCl_3 \cdot 6H_2O$. m_0=34 g; Δd_p=180–355 μm; Q=11.5 l min^{-1}; T=80°C.

behaviour in the sense that a breakpoint occurs at about z=6.3 (Fig. 4(a)). If interpreted into a chemical formula using integer number of water molecules, the composition may correspond to a $PrCl_3 \cdot 7H_2O$*$2PrCl_3 \cdot 6H_2O$-complex (i.e. $z = 6\frac{1}{3}$). Unfortunately, this clear evidence of other hydrates than integer or half fractioned numbers of crystallized water, contributes to some uncertainty to some of the other results, since in these experiments the experimental uncertainty appears to be of the order $z \pm 0.2$ and consequently may overlap two candidate hydrates (e.g., $z=3\frac{1}{3}$ or z=3). According to the authors' opinion, the first breakpoints, in Figs. 6 and 7, are particularly subjected to uncertainty and future work should find a way to determine the corresponding water numbers more precisely, either by fluidization at a lower temperature together with a more frequent sampling or by preparation by autogeneous dehydration/hydration at fixed vapor phase conditions.

In Fig. 10(a) Fig. 11(a), the breakpoints observed slightly before z=2.0 and the subsequently slow converging rate towards the dihydrated end products are of similar nature to that observed before monohydrated end products elsewhere (see Fig. 8 or [5]). The complementary experiments ('b') made for these compounds at elevated temperature show the reaction step 2→1 to follow.

All suggested dehydration schemes of this work and previously cited work are summarized in Table 2. The first column contains the suggested dehydration schemes of this work and the preceding work on Nd-, Tb- and $DyCl_3 \cdot 6H_2O$ [5]. It is to be noted that the dehydration of the monohydrate was not studied in this work. However, there seems to be no controversy in assuming this dehydration to proceed according to the reaction step 1→0.

In context, the results of the different investigators in Table 2 show a rather diverse picture of the overall dehydration scheme of rare-earth chlorides. It is difficult to make an assessment of the different results because the pertinent dehydration plots are not always included in the papers. However, the dehydration

Table 2
Reported dehydration schemes

	[5], this work	[9]	[10]	[11]	[12]	[13–15]	[16]	[17]
$LaCl_3$	7-3-1 [a]	7(-6)-3-1-0	7-3-1-0	7-3-2-1-0	7-3-1-0	7-3 [a]	3-1-0 [b]	
$CeCl_3$	7-3-2-1 [a]		7-3-2-1-0	7-3-2-1-0	7-3-2-1-0	7-4 [a]	3-2-1-0 [b]	
$PrCl_3$	7-6$\frac{1}{3}$-3-2-1 [a]		7-6-3-2-1-0	7-3-2-1-0	6-3-2-1-0	7-3 [a]		
$NdCl_3$	6-3-2-1-0		6-3-2-1-0	6-3-2-1-0	6-3-2-1-0	6-3 [a]	3-2-1-0 [b]	6-5-4-1-0
$SmCl_3$	6-3-2-1 [a]		6-3-2-1 [a]	6-4-2-1-0	6-3-2-1-0	6-3 [a]	3-2-1-0 [b]	
$EuCl_3$	6-3-2-1 [a]		6-3-2-1 [a]	6-3-2-1-0	6-3-2-1-0	6-3 [a]	3-2-1-0 [b]	
$GdCl_3$	6-3-2-1 [a]		6-3-2-1-0	6-3-2-1-0	6-3-1$\frac{1}{2}$-0	6-3 [a]	3-2-1-0 [b]	
$TbCl_3$	6-3-2-1-0		6-2-1-0	6-4-2-1-0	6-3-1-0	6-2$\frac{1}{2}$ [a]	3-2-1-0 [b]	
$DyCl_3$	6-3-1-0		6-2$\frac{1}{2}$-1-0	6-3-1-0	6-3-1-0	6-2 [a]	3-1-0 [b]	
$HoCl_3$	6-2-1 [a]		6-2-1-0	6-2-1-0	6-3-1-0	6-2 [a]		
$ErCl_3$	6-3-2-1 [a]		6-3$\frac{1}{2}$-2-1-0	6-4-2-1-0	6-3-1-0	6-3 [a]	3-2-1-0 [b]	
$TmCl_3$	6-3$\frac{1}{2}$-2-1 [a]		6-3$\frac{1}{2}$-2-1-0	6-4-2-1-0	6-3-1-0	6-3 [a]		
$YbCl_3$	6-3$\frac{1}{2}$-2-1 [a]		6-3$\frac{1}{2}$-2-1-0	6-4-2-1-0	6-3-1-0		3-2-1-0 [b]	
$LuCl_3$			6-3$\frac{1}{2}$-2-1-0	6-4-2-1-0	6-3-1-0	6-3 [a]		
YCl_3	6-2-1 [a]		6-2-1-0		6-1-0		3-2-1-0 [b]	

[a] Dehydration was only studied down to the corresponding hydrate.
[b] Dehydration was only studied from the trihydrate.

schemes of the lighter rare earths are in a better accordance than those of the heavier (Tb-Y). This is most probably due to the deviation of compositional data caused by interference from hydrolysis, which is expected to increase with the decreasing ionic radii of heavier elements. Therefore, the results of Haeseler and Matthes [10] and this work including [5] are more reliable because they are based on dehydration conducted in a HCl-containing atmosphere. Comparing these results, a total agreement of the suggested dehydration schemes is found, except for Pr-, Tb-, Dy- and $ErCl_3$. Regarding Tb- and $DyCl_3$, it is an indicative fact that the results obtained by the fluidized-bed technique [5] were very carefully elaborated, with a total number of 15 experiments for $TbCl_3$ and 26 experiments for $DyCl_3$ [6], and none of them diverged from the stated dehydration schemes. It is interesting to find that a $3\frac{1}{3}$-hydrate has been experimentally evidenced in both investigations in the case of $TmCl_3$ and $YbCl_3$. However, in the case of $ErCl_3$, Haeseler and Matthes [10] believed that $3\frac{1}{3}$-hydrate was formed, while the conclusion from this work has shown the formation of a 3-hydrate.

4. Conclusions

The dehydration schemes of rare-earth chlorides (except Sc- and $LuCl_3$) were investigated by the fluidized-bed technique. Results were interpreted from both chemical and thermal analyses. The following dehydration schemes are suggested:

$LaCl_3$: $7\rightarrow3\rightarrow1\rightarrow0$; $CeCl_3$: $7\rightarrow3\rightarrow2\rightarrow1\rightarrow0$; $PrCl_3$: $7\rightarrow6\frac{1}{3}\rightarrow3\rightarrow2\rightarrow1\rightarrow0$; $NdCl_3$: $6\rightarrow3\rightarrow2\rightarrow1\rightarrow0$; $SmCl_3$: $6\rightarrow3\rightarrow2\rightarrow1\rightarrow0$; $EuCl_3$: $6\rightarrow3\rightarrow2\rightarrow1\rightarrow0$; $GdCl_3$: $6\rightarrow3\rightarrow2\rightarrow1\rightarrow0$; $TbCl_3$: $6\rightarrow3\rightarrow2\rightarrow1\rightarrow0$; $DyCl_3$: $6\rightarrow3\rightarrow1\rightarrow0$; $HoCl_3$: $6\rightarrow2\rightarrow1\rightarrow0$; $ErCl_3$: $6\rightarrow3\rightarrow2\rightarrow1\rightarrow0$; $TmCl_3$: $6\rightarrow3\frac{1}{3}\rightarrow2\rightarrow1\rightarrow0$; $YbCl_3$: $6\rightarrow3\frac{1}{3}\rightarrow2\rightarrow1\rightarrow0$; YCl_3: $6\rightarrow2\rightarrow1\rightarrow0$.

Acknowledgements

The present work has been carried out with the financial aid of SIDA (Swedish International Development Cooperation Authority), which is gratefully acknowledged.

References

[1] J. Sundström, Preparation of $DyCl_3$ by dehydration in a fluidized bed, in: R.G. Bautista, C.O. Bounds, T.W. Ellis, B.T. Kilbourn (The Minerals, Metals and Materials Society, 1997) (Eds.), Rare Earths Science, Technology and Applications, 9–21.
[2] F. Seon, G. Barthole, Eur. Patent No. 0184515, Dec. 1985.
[3] R.A. Sharma, Eur. Patent No. 0238185, Feb. 1987.
[4] Y. Sato, M. Hara, Formation of Intermetallic Compounds Layer Composed of Ni_3Y and Ni_5Y by Electrodeposition on Ni Using Molten NaCl-KCl-YCl_3, Materials Transactions, JIM 37 (1996) 1525.
[5] J. Sundström, O. Wijk, Investigation of the dehydration schemes of $NdCl_3{\cdot}6H_2O$, $TbCl_3{\cdot}6H_2O$ and $DyCl_3{\cdot}6H_2O$ using a fluidized bed, (Paper presented at the 21st Rare Earth Research Conference, Duluth, Minnesota, 7–12 July 1996). To be published in JALCOM.
[6] J. Sundström, V.V. Hong, to be published in this Journal.
[7] W.W. Wendlandt, J. Inorg. Nucl. Chem. 5 (1957) 118.
[8] W.W. Wendlandt, J. Inorg. Nucl. Chem. 9 (1959) 136.
[9] J.E. Powell, H.R. Burkholder, J. Inorg. Chem. 14 (1960) 65.
[10] G. Haeseler, F. Matthes, J. Less-Com. Met. 9 (1965) 133 (in German).
[11] S.J. Ashcroft, C.T. Mortimer, J. Less-Comm. Met. 14 (1968) 403.
[12] M. Su, G. Li, Hua Hsueh Tung Pao, 4 (1979) 322 (in Chinese).
[13] É. Ukraintseva, A.N.P. Sokolova, V.A. Logvinenko, Soviet Radiochemistry 29 (1987) 464.
[14] É. Ukraintseva, A.N.P. Sokolova, V.A. Logvinenko, Soviet Radiochemistry 31 (1989) 4.
[15] É. Ukraintseva, A.N.P. Sokolova, V.A. Logvinenko, Soviet Radiochemistry 34 (1992) 521.
[16] J. Wang, Z. Guo, Y. Chen, S. Huang, Z. Wang, J. Northwest University, 20 (1990) 49 (in Chinese).
[17] G.J. Kipouros, R.A. Sharma, J. Less-Comm. Met. 160 (1990) 85.